JOURNAL OF VIROLOGY, Dec. 2010, p. 12576–12588 Vol. 84, No. 24
0022-538X/10/$12.00 doi:10.1128/JVI.01310-10


# Genomic Profiling of Tumor Necrosis Factor Alpha (TNF-α) Receptor and Interleukin-1 Receptor Knockout Mice Reveals a Link between TNF-α Signaling and Increased Severity of 1918 Pandemic Influenza Virus Infection▽†

Sarah E. Belisle,[1,2] Jennifer R. Tisoncik,[1,2] Marcus J. Korth,[1,2] Victoria S. Carter,[1,2] Sean C. Proll,[1,2] David E. Swayne,[3] Mary Pantin-Jackwood,[3] Terrence M. Tumpey,[4] and Michael G. Katze[1,2]*

*Department of Microbiology[1] and Washington National Primate Research Center,[2] University of Washington, Seattle, Washington 98195; Southeast Poultry Research Laboratory, Agricultural Research Laboratory, U.S. Department of Agriculture, Athens, Georgia 30606[3]; and Influenza Division, Centers for Disease Control and Prevention, Atlanta, Georgia 30333[4]*

Received 20 June 2010/Accepted 28 September 2010

**The influenza pandemic of 1918 to 1919 was one of the worst global pandemics in recent history. The highly pathogenic nature of the 1918 virus is thought to be mediated in part by a dysregulation of the host response, including an exacerbated proinflammatory cytokine response. In the present study, we compared the host transcriptional response to infection with the reconstructed 1918 virus in wild-type, tumor necrosis factor (TNF) receptor-1 knockout (TNFRKO), and interleukin-1 (IL-1) receptor-1 knockout (IL1RKO) mice as a means of further understanding the role of proinflammatory cytokine signaling during the acute response to infection. Despite reported redundancy in the functions of IL-1β and TNF-α, we observed that reducing the signaling capacity of each of these molecules by genetic disruption of their key receptor genes had very different effects on the host response to infection. In TNFRKO mice, we found delayed or decreased expression of genes associated with antiviral and innate immune signaling, complement, coagulation, and negative acute-phase response. In contrast, in IL1RKO mice numerous genes were differentially expressed at 1 day postinoculation, including an increase in the expression of genes that contribute to dendritic and natural killer cell processes and cellular movement, and gene expression profiles remained relatively constant at later time points. We also observed a compensatory increase in TNF-α expression in virus-infected IL1RKO mice. Our data suggest that signaling through the IL-1 receptor is protective, whereas signaling through the TNF-α receptor increases the severity of 1918 virus infection. These findings suggest that manipulation of these pathways may have therapeutic benefit.**

The 1918 Spanish influenza pandemic was one of the worst global pandemics in recent history, resulting in an estimated 50 million deaths worldwide (13). Studies using the reconstructed 1918 virus (r1918) (31) have shown that the highly pathogenic nature of the virus may be in part due to a dysregulation of the host response following infection (6, 7, 14, 18). In particular, our previous studies using a mouse infection model showed that the early and extensive pulmonary damage following r1918 virus infection is accompanied by a dramatic elevation in proinflammatory gene expression which occurs as early as 1 day after inoculation and is sustained until the death of the animal (14). This finding, combined with studies showing that elevated proinflammatory cytokine protein levels correlated with the severity of highly pathogenic influenza virus infection in animals and humans (1, 8, 14, 18), suggests that an augmented proinflammatory cytokine response ("cytokine storm") may contribute to fatal outcome in r1918 influenza virus infection.

Interleukin-1β (IL-1β), IL-1α, and tumor necrosis factor alpha (TNF-α) are proinflammatory cytokines that mediate the host response to infection through both direct and indirect mechanisms (reviewed in references 9 and 12). Among their biological functions, these cytokines increase acute-phase signaling, trafficking of immune cells to the site of primary infection, epithelial cell activation, and secondary cytokine production. The generation of mice that lack functional signaling through cytokine receptors makes it possible to study how the host response to influenza virus infection may be influenced by specific cytokine signaling.

In the present study, we infected wild-type (WT), IL-1 receptor 1 (IL-1R1) knockout (IL1RKO), and TNF-α receptor knockout (TNFRKO) mice with r1918 virus to better understand the interplay of IL-1- and TNF-α-mediated proinflammatory cytokine pathways in modulating the host response to infection. Although these mice are viable and fertile, reduced responses to chemical or bacterial challenge have been described in both strains of these knockout mice. IL1RKO mice have lower levels of circulating acute-phase proteins following turpentine injection, mount lower hypersensitivity responses, and are more susceptible to *Listeria monocytogenes* than WT mice (20). TNFRKO mice have normal levels of acute-phase proteins in the liver following lipopolysaccharide (LPS) injec-

* Corresponding author. Mailing address: Department of Microbiology, University of Washington, Box 358070, Seattle, WA 98195-8070. Phone: (206) 732 6135. Fax: (206) 732 6056. E-mail: honey@u.washington.edu.

† Supplemental material for this article may be found at http://jvi.asm.org/.

▽ Published ahead of print on 6 October 2010.

tion, are less susceptible to septic shock induced by LPS and D-Gal, and exhibit a decrease in neutrophil infiltration in the lungs following *Micropolyspora faeni* challenge despite normal monocyte and lymphocyte infiltration (25).

Previous studies of H5N1 avian influenza virus in TNFRKO mice suggest that TNF-α signaling confers accelerated morbidity (30). In contrast, studies of H5N1 avian-origin and H1N1 influenza viruses in IL1RKO mice suggest that IL-1R1 signaling increases the damage to the lungs following infection despite slowing mortality (27, 30). In the present study, we used high-throughput gene expression profiling to evaluate the global host response to r1918 virus infection in these animals and found that signaling through IL-1R1 and TNFR had distinct effects on the acute-phase response, inflammation mediated through TREM1 (triggering receptor expressed on myeloid cells), cell movement, and antiviral innate immune responses. These differences in the transcriptional response may contribute to the differential severity of disease observed in IL1RKO and TNFRKO mice and suggest that TNFR signaling is a key factor contributing to the severity of r1918 virus infection.

## MATERIALS AND METHODS

**Mice.** Age-matched (6- to 7-week old) wild-type (C57B6/129SF2J), IL1RKO (B6;129S1-*Il1r1*$^{tm1Roml}$), and TNFRKO (B6;129S-*Tnfrsf1a*$^{tm1Imx}$*Tnfrsf1b*$^{tm1Imx}$) mice were obtained from Jackson Laboratory (Bar Harbor, ME). Animal research was conducted under the guidance of the CDC's Institutional Animal Care and Use Committee in an animal facility accredited by the Association for Assessment and Accreditation of Laboratory Animal Care International.

**Viral challenge.** The reconstructed 1918 (abbreviated r1918) virus used in this study is described in detail in Tumpey et al. (31). Mice were anesthetized with Avertin (Sigma-Aldrich, St. Louis, MO) and infected intranasally (i.n.) (50 μl) with $10^6$ PFU of r1918 virus. Whole lungs were harvested at 1, 3, and 5 days postinoculation (dpi) for viral titration, histopathology, and extraction of total RNA. Body weight was measured at 0, 2, 4, 6, and 8 dpi, and survival was recorded until 10 dpi. All animal work was performed in a specially separated negative-pressure high-efficiency particulate air (HEPA)-filtered biosafety level laboratory 3 (BSL3) with enhancements.

**Statistical analysis of virological data.** One-way analysis of variance (ANOVA) was used to determine differences in viral titer and body weight between strains on each day postinoculation. A Tukey-Kramer honestly significant difference (HSD) posthoc adjustment was applied to determine the pairwise differences in measures between mouse strains. Differences in survival were determined using product-limit survival fit with log rank tests to determine differences between strains. Statistical comparisons for virology data were performed with JMP statistical software (version 6; SAS Institute Inc., Cary, NC).

**Histopathology.** Three mice from each group were euthanized at 1, 3, and 5 dpi. A 5-mm lung piece from the ventral end of each left lobe was collected for histopathology. Pathological changes were evaluated in the lungs of all mice at the time of necropsy. Tissue samples were fixed in 10% neutral phosphate-buffered formalin, sectioned using a diamond-edge microtome, routinely processed, and stained with hematoxylin and eosin (H&E) following standard protocols. Duplicate sections were stained by immunohistochemistry methods to determine virus antigen distribution in lung tissues. The sections were first heated in a microwave oven in Antigen Retrieval Citra Solution (Biogenex, San Ramon, CA) for antigen exposure. A 1:2,000 dilution of a mouse-derived monoclonal antibody (P13C11) specific for a type A influenza virus nucleoprotein was applied and allowed to incubate for 12 h at 4°C. The primary antibody was then detected by the application of biotinylated goat anti-mouse IgG secondary antibody using the Mouse-on-Mouse System (Vector Laboratories, Inc., Burlingame, CA) as per the manufacturer's instructions. An AEC (3-amino-9-ethylcarbazole) peroxidase substrate kit (Vector Laboratories, Inc.) was used as the substrate chromogen, and hematoxylin was used as a counterstain.

**Total RNA isolation and RNA amplification.** Lung samples were stored in solution D (4 M guanidinium thiocyanate, 25 mM sodium citrate, 0.5% sarcosyl, 0.1 M β-mercaptoethanol) (5) at −80°C until processing. Tissues were then homogenized in solution D for at least 30 s (or until completely homogenized) with a Kinematica Polytron PT1200 instrument. The homogenized material was transferred to a fresh 15-ml tube and brought to a total volume of 15 ml with ice-cold solution D. Added to this were 650 μl of 2 M sodium acetate, 6.5 ml of water-saturated phenol, and 1.3 ml of chloroform-isoamyl alcohol (49:1). Tubes were vortexed and then centrifuged for 30 min at 8,500 rpm at 4°C using a Beckman L8-80 M ultracentrifuge with a JA18 rotor. The resulting aqueous layer was extracted and transferred to a fresh tube and precipitated with an equal volume of ice-cold isopropanol at −20°C overnight. Following centrifugation, as described above, the resulting pellet was rinsed in 75% ethanol and resuspended in 150 μl of RNase-free water.

**Expression microarray analysis and bioinformatics.** Total RNA isolation and mRNA amplification were performed on equal masses of total RNA isolated from lungs of infected mice and were compared with an equal-mass pool of RNA from lungs of individual mock-infected mice. Reverse transcription-PCR (RT-PCR) was performed on RNA isolated for array analysis using probes against a consensus region of the matrix gene, as determined based on three H1N1 influenza virus strains (A/pintail duck/Alberta/210/2002, A/mallard/Alberta/130/2005, and A/mallard/Alberta/267). This was performed to confirm the presence of influenza virus in the lung samples analyzed for gene expression.

Expression oligonucleotide arrays were performed on RNA isolated from lung tissue from three individual animals per group at days 1, 3, and 5 postinoculation ($n = 2$ technical replicates per mouse). Probe labeling and microarray slide hybridization were performed with a Mouse V2 Oligo Microarray (G4121B; Agilent Technologies). All data were entered into a custom-designed Oracle 9i-backed relational database and then uploaded into Rosetta Resolver System, version 5.0 (Rosetta Biosoftware), and Spotfire Decision Site, version 8.1 (Spotfire). All primary expression microarray data, in accordance with the proposed minimum information about a microarray experiment (MIAME) standards (3), are available at http://viromics.washington.edu.

A Student's one-sample $t$ test ($P \leq 0.01$) was performed to determine the genes that had significantly different expression levels with infection compared to levels in mock infections on each day postinoculation for each of the three mouse strains. One-way ANOVA was used to determine differences in gene expression between strains on each day postinoculation (ANOVA, $P < 0.01$); genes that specifically distinguished the strains from each other were determined by applying a Student's posthoc test ($P < 0.1$) to ANOVA results. To select for genes that were most relevant to infection, the genes that were differentially expressed between strains on a given day were filtered to include only the genes that were significantly different from genes expressed in mock infections in at least one of the strains being compared on that day postinoculation and that were different from mock infections by at least a 1.5-fold change in one of the strains being compared.

Functional analysis of statistically significant gene expression changes was performed with Ingenuity Pathways Analysis (IPA; Ingenuity Systems). This software analyzes RNA expression data in the context of known biological response and regulatory networks as well as other higher-order response pathways. Ingenuity functional analysis identified biological functions and/or diseases that were most significant. For all analyses, a Benjamini-Hochberg test correction was applied to the IPA-generated $P$ value to determine the probability that each biological function assigned to that data set was due to chance alone. In the functional networks, genes are represented as nodes, and the biological relationship between two nodes is represented as an edge (line). All edges are supported by at least one published reference or from canonical information stored in the Ingenuity Pathways Knowledge Base.

## RESULTS

**r1918 virus-induced weight loss, time to death, and pathology are dependent upon mouse genotype.** WT ($n = 19$), IL1RKO ($n = 12$), and TNFRKO ($n = 13$) mice were infected i.n. with $10^6$ PFU of r1918 virus, and weight loss and mortality were monitored for 8 and 10 dpi, respectively. WT and IL1RKO mice exhibited significant and sustained weight loss as early as 1 dpi and weighed significantly less than the TNFRKO mice at all time points ($P < 0.05$) (Fig. 1A). In contrast, weight loss was not consistently observed in all TNFRKO mice until 6 dpi, at which point the TNFRKO mice achieved statistically significant weight loss ($P < 0.05$). Median time to death was longer for TNFRKO mice (8 dpi) than for WT (7 dpi) or IL1RKO mice (6 dpi) (Fig. 1B). The differences

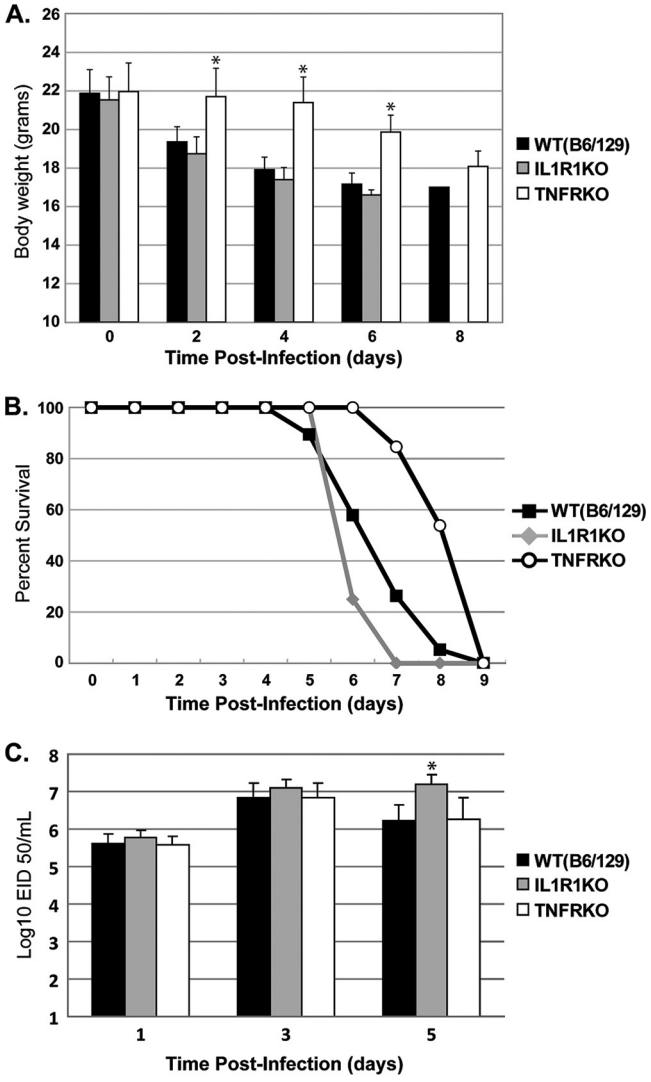


FIG. 1. Characterization of mortality, weight loss, and lung viral titers in r1918-infected WT, TNFRKO, and IL1RKO mice at 1, 3, and 5 dpi. (A) Average weight of surviving animals at each time point (expressed as mean ± standard deviation SD; $n = 6$ for TNFRKO and IL1RKO, and $n = 9$ for WT). (B) Survival of animals was monitored in animals ($n = 13$ for TNFRKO, $n = 12$ for IL1RKO, and $n = 19$ for WT) following intranasal inoculation with the r1918 virus. (C) Influenza virus titers measured in the lungs at 1, 3, and 5 dpi ($n = 6$ for TNFRKO and IL1RKO; $n = 9$ for WT). Differences between group means for weight and titer were determined by Tukey-Kramer HSD posthoc analysis of one-way ANOVA results ($P < 0.05$); groups with statistically significant differences are denoted with an asterisk. EID 50, 50% egg infectious dose.

in time to death between the WT and IL1RKO mice did not reach statistical significance ($P = 0.06$); however, the TNFRKO mice statistically survived longer than the WT ($P = 0.0005$) and IL1RKO mice ($P < 0.0001$).

Viral titer in the lungs of infected animals was measured at 1, 3, and 5 dpi ($n = 6$ for TNFRKO and IL1RKO mice; $n = 9$ for WT mice). There were no significant differences in viral titers in the lungs at 1 and 3 dpi between the three mouse strains (Fig. 1C). However, IL1RKO mice had higher levels of virus in the lung than WT and TNFRKO mice at 5 dpi ($P < 0.05$). Although it is difficult to concretely determine if this is biologically significant, the occurrence of earlier mortality within the IL1RKO mice suggests that this difference in viral load may be biologically relevant. Viral titers were not measured in the blood. However, virus was not detected in the brain or spleen of any of the mice at any of the time points examined, suggesting that the virus did not become systemic in these animals at this inoculation dose (data not shown). Virus replication in the lungs of infected mice was confirmed by real-time, quantitative RT-PCR (qRT-PCR) with probes specific to the influenza virus matrix gene (data not shown).

Histopathology was examined by hematoxylin and eosin staining of lung tissue sections from infected animals, and viral antigen was detected by immunohistochemistry (Fig. 2). We found that at 1 dpi, WT mice either lacked airway lesions or had mild epithelial cell degeneration, but they had mild diffuse histiocytic alveolitis with some perivascular cuffs of neutrophils and lymphocytes. No viral antigen staining was detected in lung and airway samples at this time point (Fig. 2A). At 3 and 5 dpi, moderate necrotizing bronchiolitis and bronchitis with associated neutrophilic to histiocytic luminal and peribronchiolar inflammation were present, accompanied by mild to moderate diffuse histiocytic to neutrophilic alveolitis. Viral antigen was commonly seen in respiratory epithelium of the upper and lower airways and, slightly less commonly, within peribronchiolar alveolar macrophages (Fig. 2B). Viral antigen staining declined slightly at 5 dpi in the airway epithelium.

TNFRKO mice at 1 dpi had mild to moderate necrosis in bronchi and bronchioles, with minimal to no associated inflammation and mild to moderate peribronchiolar histiocytic to neutrophilic alveolitis. Viral antigen was infrequent in respiratory epithelial cells and rare in alveolar macrophages (Fig. 2C). At 3 and 5 dpi, in comparison to the lungs from WT mice, the necrosis in TNFRKO mice was progressively less prominent, and inflammation was minimal or lacking (Fig. 2D). On day 3, viral antigen staining in TNFRKO mice was less severe than in WT mice (Fig. 2D insert), and on day 5, minimal viral antigen was detected, less than in any of the other mouse groups.

IL1RKO mice had mild to moderate necrosis in bronchi and bronchioles at 1 dpi with associated heterophilic to histiocytic inflammation and mild peribronchiolar histiocytic alveolitis. Viral antigen was commonly seen in degenerating or necrotic respiratory epithelium of the pulmonary bronchioles and associated luminal debris and frequently within alveolar epithelium and alveolar macrophages (Fig. 2E). At 3 and 5 dpi, the necrosis and inflammation in IL1RKO mice were slightly less severe than at 1 dpi but much less severe than in the corresponding WT mice. The IL1RKO mice had similar alveolar and airway lesions at 1 and 3 dpi as TNFRKO mice except that the histiocytic alveolitis was only peribronchiolar and was less severe in the IL1RKO mice. At 3 dpi, viral antigen was present in necrotic cellular debris within bronchiolar lumina and especially in alveoli and alveolar macrophages. Virus-positive respiratory epithelial cells were less frequently observed than at 1 dpi (Fig. 2F). At 5 dpi, the IL1RKO mice retained mild to moderate lesions in alveoli and airways while such lesions were reduced in TNFRKO mice.

In summary, at 1 dpi, pathology and viral antigen detection were greatest in IL1RKO and TNFRKO mice and least in WT animals. However, at 3 and 5 dpi, pathology continued to

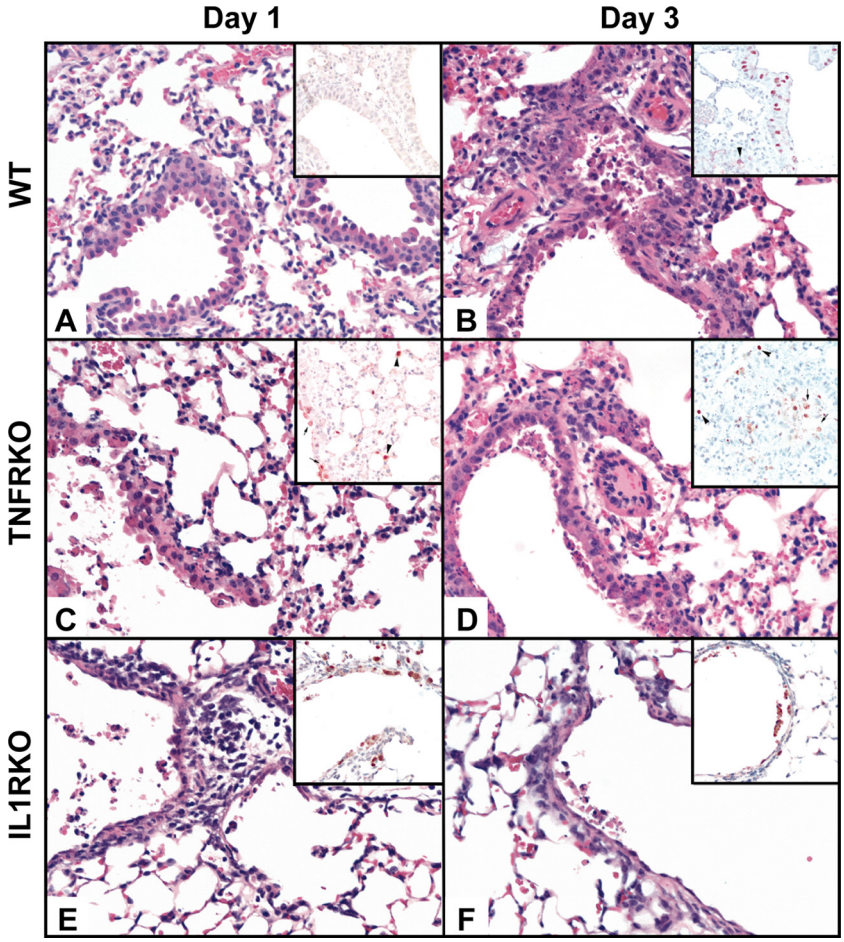


FIG. 2. Photomicrographs of hematoxylin-and-eosin-stained and immunohistochemically stained lung tissue sections from mice intranasally inoculated with r1918 virus. (A) Mild epithelial cell degeneration and associated mild histiocytic alveolitis in WT mouse at 1 dpi. (Inset) Lack of viral antigen staining in lung. (B) Moderate necrosis of bronchiolar epithelial cells and associated mild peribronchiolar histiocytic alveolitis with edema in WT mice at 3 dpi. (Inset) Viral antigen was common in bronchiolar epithelial cells and occasionally in alveolar macrophages (arrowhead). (C) Moderate necrosis in bronchiolar epithelial cells with mild alveolitis and edema in TNFRKO mouse at 1 dpi. (Inset) Viral antigen in bronchiolar epithelial cells (arrows) and alveolar macrophages (arrowheads). (D) Mild epithelial cell necrosis in bronchiole with some necrotic luminal debris and minimal peribronchiolar inflammation in TNFRKO mouse at 3 dpi. (Inset) Infrequent viral antigen in respiratory epithelial cells of bronchioles (arrows) and in alveolar macrophages (arrowheads). (E) Moderate necrosis of bronchiolar epithelial cells with mild peribronchiolar inflammation and alveolitis with edema in IL1RKO mouse at 1 dpi. (Inset) Viral antigen was common in respiratory epithelial cells of bronchiole, luminal necrotic debris, and frequent in alveolar macrophages. (F) Early regenerating epithelial cells in bronchiole with some luminal necrotic debris and mild peribronchiolar inflammation in IL1RKO mouse at 3 dpi. (Inset) Viral antigen in necrotic debris within bronchiolar lumen.

increase in WT mice but became less severe in IL1RKO mice. TNFRKO mice exhibited an intermediate level of pathology at 3 dpi and the least amount of pathology and viral antigen at the later time points. Overall, these histopathological findings are consistent with the reduced amount of weight loss and the longer median time to death observed for TNFRKO mice. Although it is not clear why the IL1RKO mice exhibited less pathology at 3 and 5 dpi and died sooner than the WT mice, this observation has been previously reported (27, 30). It is possible that, although the damage lessened over time, the IL1RKO mice were not able to recover from the overwhelming, early tissue damage.

**IL1RKO and TNFRKO mice exhibit dramatic differences in global gene expression in response to infection.** To better understand the role of IL-1R1 and TNFR signaling in the host response to r1918 virus infection, we examined global gene expression within the lungs of infected animals at 1, 3, and 5 dpi. We observed that IL1RKO mice had the greatest number of genes differentially expressed in response to infection and that a large number of these genes were differentially expressed at each time point (Table 1). In contrast, fewer genes were differentially expressed in WT and TNFRKO mice across these time points, and the number, identity, and relative expression of differentially expressed genes were more variable. This suggests that IL-1R1 signaling may be required for effective modulation of the host transcriptional response over time.

In all three strains of mice at all three time points, a significant number of differentially expressed genes were related to cell death (32 to 38% of genes with annotation) and cellular growth and proliferation (28 to 42% of genes with annotation) (see Table S1 in the supplemental material). When we examined the genes that increased with infection separately from

TABLE 1. Number of genes differentially expressed in the lungs of mice infected with r1918 virus

| Day postinoculation | No. of differentially expressed genes (% upregulated)[a] | | |
|---|---|---|---|
| | WT | IL1RKO | TNFRKO |
| 1 | 1,005 (51) | 5,550 (50) | 1,911 (50) |
| 3 | 1,717 (60) | 5,359 (50) | 3,526 (45) |
| 5 | 2,324 (52) | 5,048 (55) | 2,442 (44) |
| Total | 65 | 2,417 | 504 |

[a] Differential expression was determined for WT (B6/129), IL1RKO, and TNFRKO mice by a Student's one-sample *t* test ($P \leq 0.01$) of the ratio of gene expression for r1918-infected versus mock-infected samples at each time point ($n = 3$ per strain per time point). For each strain, the expression of each of the differentially expressed genes was compared between the r1918 virus and matched mock groups.

TABLE 2. Top canonical pathways distinguishing TNFRKO mice from IL1RKO and WT mice at each day postinfection

| Day | IPA canonical pathway[a] | B-H *P* value[b] |
|---|---|---|
| 1 | Acute-phase response signaling | 0.045 |
| 3 | Acute-phase response signaling | 0.003 |
| | ILK signaling | 0.012 |
| | LPS/IL-1 mediated inhibition of RXR function | 0.033 |
| | Complement system | 0.038 |
| | Aryl hydrocarbon receptor signaling | 0.038 |
| | Hepatic fibrosis/hepatic stellate cell activation | 0.048 |
| | Production of nitric oxide and reactive oxygen species in macrophages | 0.048 |
| 5 | DC maturation | 0.002 |
| | Hepatic fibrosis/hepatic stellate cell activation | 0.006 |
| | Role of PKR in IFN induction and antiviral response | 0.008 |
| | IL-4 signaling | 0.008 |
| | Activation of IRF by cytosolic pattern recognition receptors | 0.018 |
| | Fcγ receptor-mediated phagocytosis in macrophages and monocytes | 0.020 |
| | Interferon signaling | 0.020 |
| | Role of pattern recognition receptors in recognition of bacteria and viruses | 0.021 |
| | Production of nitric oxide and reactive oxygen species in macrophages | 0.036 |
| | TREM1 signaling | 0.043 |
| | Cross talk between DC and NK cells | 0.043 |

[a] Top pathways were determined using IPA of genes that were different by ANOVA using posthoc comparisons to determine pairwise differences in gene expression at each time point; IRF, IFN regulatory factor.
[b] A Benjamini-Hochberg (B-H) test correction was applied to significance values for each pathway.

those that decreased, we observed an increase in inflammatory response, cell death, cell growth and proliferation, and hematological system development and function. Further, there was a decrease in the transcription of genes related to lipid metabolism and small-molecule biochemistry in all three strains of mice at the time points examined. These common biological responses to the r1918 virus may be in part due to the increase in immune cell recruitment and tissue remodeling occurring in the lung. However, although the three mouse strains had altered expression levels of genes within these categories, the expression patterns of genes also showed unique differences in the precise genes regulated, the extent of differential expression, or the kinetics of the response (see Table S2).

To address whether differences in the response to the r1918 virus in the three strains might be due to patterns of cytokine gene expression, we next examined differential cytokine expression across 1, 3, and 5 dpi (see Fig. S1 in the supplemental material). In contrast to what might be expected under the general hypothesis of a cytokine storm, we observed that overall patterns of expression for these genes were similar between the WT and TNFRKO mice. In contrast, IL1RKO mice exhibited an increase in the expression of many chemokines (TNF-α, gamma interferon [IFN-γ], and IFN-β), which occurred earlier than in the WT or TNFRKO mice. This suggests that absence of IL-1R1 signaling has a more widespread impact on cytokine expression than the absence of TNFR signaling. However, the similarities in expression between the WT and TNFRKO mice also indicated that expression of other genes may be influencing differences in the phenotypes observed in these mice.

**IL-1R1 and TNFR have distinct roles in complement and coagulation response.** To gain insight into why TNFRKO mice were able to live longer than WT and IL1RKO mice and maintain their body weight, we next performed pairwise comparisons of gene expression at 1, 3, and 5 dpi to determine the gene expression patterns that specifically distinguished TNFRKO mice from the other mouse strains. From this analysis, we identified 383 genes at 1 dpi, 1,056 genes at 3 dpi, and 905 genes at 5 dpi that distinguished the TNFRKO mice from the other two stains. Functional analysis of these genes suggests distinct regulation of several biological pathways within the TNFRKO animals which may contribute to decreased pathology and increased time to death (Table 2). For example, TNFRKO mice exhibited an expression profile for genes associated with acute-phase signaling that distinguished them from the other two mouse strains at 1 and 3 dpi. Activation of acute-phase signaling results in a range of biological activities in response to viral infection, including many inflammatory processes. Acute-phase signaling is particularly relevant to the present study because signaling through the pathway is initiated by TNFR, IL-1R1, and IL-6 expression (reviewed in reference 10). When we compared the genes that were differentially expressed in TNFRKO mice with genes differentially expressed in the other two strains, we identified genes downstream of all three cytokine receptors (IL-1R1, TNFR, or IL-6R) that had unique expression patterns in the TNFRKO mice (Fig. 3; see also Fig. S2 in the supplemental material). The alteration of gene expression downstream of IL-1R1 and IL-6R in TNFRKO mice suggests that the loss of TNFR signaling during infection has a substantial impact on acute-phase signaling, including an impact on signaling mediated through these receptors.

We next expanded our view of acute-phase signaling beyond what was specifically different in the TNFRKO mice. As shown in blue in Fig. 3, the majority of genes within the pathway were differentially expressed between strains on at least one time point. This included an upregulation of negative acute-phase response genes in WT mice at 1 and 3 dpi that was not observed in the knockout animals (Fig. 4). This finding suggests that both IL-1 and TNF-α signaling are required for the increased expression of these genes following r1918 infection. It

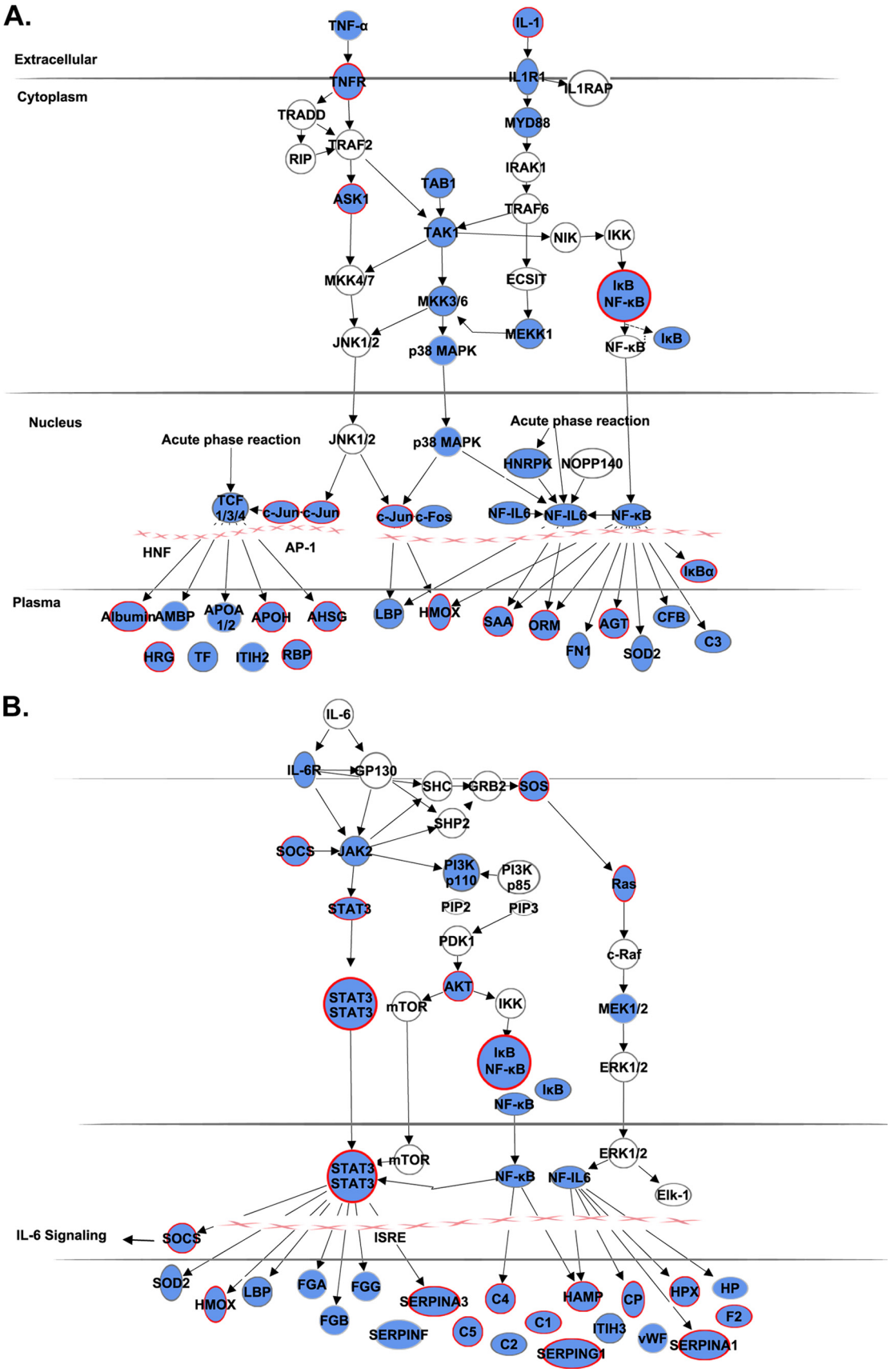


FIG. 3. Differential host transcriptional responses within the acute-phase response pathway in r1918-infected WT, TNFRKO, and IL1RKO mice at 1, 3, and 5 dpi. Diagram shows the acute-phase response signaling pathway including cascades initiated through the TNF-α receptor and IL-1 receptor (A) and the IL-6 receptor (B). Molecules in blue were differentially expressed between mouse strains on at least 1 dpi. Molecules outlined in red distinguished the TNFRKO mice from both WT and IL1RKO mice on at least 1 dpi based on posthoc analysis of ANOVA results.

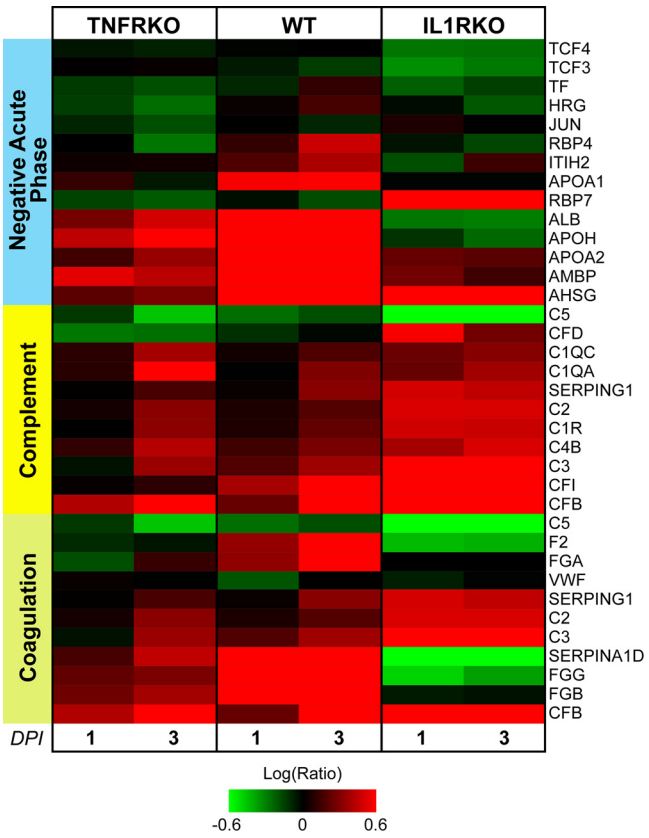


FIG. 4. Differential activation of acute-phase response signaling pathways in r1918-infected WT, TNFRKO, and IL1RKO mice. One-dimensional clustering of differentially expressed genes within the categories of negative acute-phase molecules, complement, and coagulation pathways. Genes that were differentially expressed between mouse strains on at least 1 dpi were selected for representation in the negative acute-phase and coagulation clusters from within the acute-phase canonical pathways. Complement-related molecules were selected from the acute-phase response and complement canonical pathways. Select molecules play roles in both coagulation and complement and are shown in both categories. Average expression for each group is shown as the log(ratio) of expression relative to a pool of RNA extracted from lungs of mock-infected mice, matched for genetic background to each strain. Red indicates that the gene expression is higher than that in the uninfected reference; green indicates that gene expression is lower than that in the uninfected reference sample. Clustering was performed using the hierarchical unweighted-pair group method using average linkages (UPGMA) with a Euclidean distance similarity measure and average value ordering function.

is notable that the relative decrease in negative acute-phase molecule gene expression in the IL1RKO mice coincided with a decrease in the expression of TCF3 and TCF4, transcription factors that regulate the expression of genes that code for negative acute-phase molecules including apolipoproteins (11). This may be one potential mechanism by which the animals in this group suppress the expression of negative acute-phase response genes.

An increase in complement expression is a downstream consequence of acute-phase response signaling. We found that genes associated with the complement canonical pathway generally had lower expression in TNFRKO mice than in the IL1RKO and WT animals, particularly at 3 dpi (Table 2), and the highest expression in the IL1RKO mice on all 3 days (Fig. 4). One exception to this trend was the marked decrease in the expression of the complement protein C5 gene in the IL1RKO mice across 1, 3, and 5 dpi. Although the expression of the C5 gene was also decreased in the WT and TNFRKO mice compared to expression in uninfected mice, this decrease in expression was not apparent until 3 and 5 dpi in the TNFRKO mice and 5 dpi in the WT mice. This suggests that IL-1R1 signaling plays a role in the relative repression of complement genes following r1918 virus infection. The differential impact of IL-1R1 and TNFR signaling on complement is interesting in light of recent of work indicating a role for complement in the activation and infiltration of influenza virus-specific T cells in the lung during infection (17, 19, 21).

The regulation of coagulation is closely linked to complement, and we also identified a delay in (fibrinogen B [FGB] and SERPINA1) or relative absence of differential expression (F2, FGA, and SERPING1) of coagulation genes in the TNFRKO mice at 1 and 3 dpi compared to WT (Fig. 4). This suggests that the initiation of the coagulation response may be one mechanism by which TNFR signaling impacts the severity of influenza virus infection. This was distinct from IL-1R1 signaling, as all of these molecules and the coagulation-associated gene FGG were notably downregulated or unchanged compared to their levels in mock infections in the IL1RKO mice.

**TNFRKO mice exhibit a lower specific antiviral and innate immune response.** Expression of a highly interconnected network of interferon-related antiviral genes was significantly lower in TNFRKO mice than in WT and IL1RKO mice at 5 dpi (Fig. 5A). When we examined the temporal expression patterns of genes in this network, we found that their expression increased in the context of infection for each strain. To understand how the extent of upregulation of this network differed between mouse strains, we calculated the average change in expression for this network by taking the change in expression for all molecules at each day postinoculation and dividing this number by the number of molecules within the network. This indicated that the average expression of genes within the network was lower in the TNFRKO mice than in the other two strains (Fig. 5B). This could be due in part to the relative absence of signaling through TNF receptor (TNFRSF1a) to STAT1 in the TNFRKO mice. It is of note that the IL1RKO mice had the highest average expression level of these molecules, and this degree of upregulation was maintained over time. Combined, these data suggest that TNFRKO mice have a delayed or decreased transcriptional response within key pathways, including antiviral and innate immune signaling, complement, coagulation, and regulation of negative acute-phase response genes. The differential regulation of these host responses within the TNFRKO mice suggest several mechanisms by which TNFR signaling influences the degree of tissue damage and the survival time in mice infected with the r1918 virus.

**IL1RKO mice exhibit enhanced inflammatory and dendritic cell (DC)-related gene expression at 1 dpi.** We next examined the transcriptional pathways specifically impacted by the loss of IL-1R1 signaling during r1918 virus infection to understand why the IL1RKO mice died sooner than the other mouse strains. This was done by evaluating the genes that were uniquely expressed in the IL1RKO mice using pairwise comparisons of the one-way ANOVA ($P < 0.05$) between IL1RKO

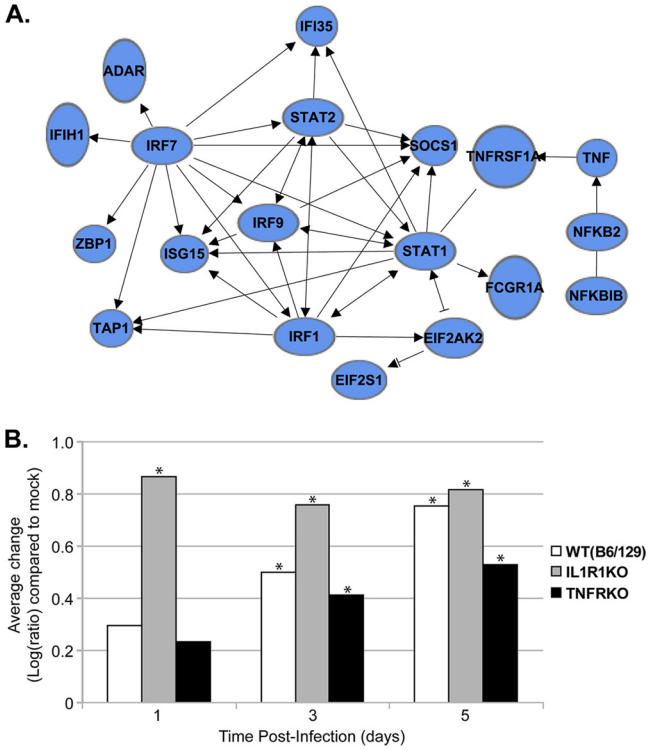


FIG. 5. Differential gene expression of interferon-related innate responses distinguishes TNFRKO mice from WT and IL1RKO strains during r1918-infection. (A) IPA of gene expression differences that distinguished TNFRKO from WT and IL1RKO mice at each time point by ANOVA and posthoc comparisons determined an enrichment of genes within three interferon-related signaling pathways which are highly interconnected. (B) Average change in expression within this network was calculated for each mouse strain on each day postinoculation by dividing the sum of changes in expression compared to expression in mock infections for each of the molecules in the network by the number of molecules in the network. The change in expression is represented as the log(ratio) of expression compared to matched mock values. Differences between group means were determined by Fisher's posthoc analysis of one-way ANOVA results ($P < 0.05$), with statistically significant differences denoted with an asterisk.

mice and WT mice and between IL1RKO mice and TNFRKO mice at 1, 3, and 5 dpi.

At 1 dpi, a significant proportion of the genes related to immune cell trafficking and cell-to-cell signaling interactions distinguished IL1RKO mice from the other two mouse strains. These included genes that regulate intercellular communication between DC and NK cells, TREM1 signaling, and DC maturation (Table 3). Within the TREM1 pathway, molecules that mediate pathogen recognition and subsequent inflammation (TREM1, NOD2, and TYROBP) (2, 22, 26) and chemoattractant molecules (MIP-1α, MCP-1, and MCP-3) had the highest expression in IL1RKO mice among all mouse strains (Fig. 6A). In the IL1RKO mice, these changes were concurrent with a downregulation of TREM2, which suppresses TNF-α, thereby promoting an anti-inflammatory state (32). Concurrent with TREM1 signaling activation was the upregulation of genes related to DC maturation and communication between DC and NK cells, including killer cell lectin-like receptors (KLRK1 and KLRD1) and molecules associated with the activation of T cells (IFN-γ, CD86, and ICAM-1) at 1 dpi.

Many of the molecules related to DC function and TREM1 signaling form an interconnected network (Fig. 6B), and TNF-α is a central molecule within these three pathways. Although expression of TNF-α is increased in the other strains, the expression of the TNF-α gene was upregulated to the greatest extent in the IL1RKO mice, specifically distinguishing the IL1RKO mice from the other strains at all time points measured. This may suggest that in the absence of IL-1R1 signaling the IL1RKO mice disproportionally increase TNF-α gene expression, perhaps reflecting a level of redundancy in proinflammatory response. Increased expression of TREM1 and increased inflammation and cell-specific responses at 1 dpi correlate with the greater degree of inflammation noted in the lungs of IL1RKO mice at 1 dpi by histopathology.

**IL1RKO mice exhibit increased expression of cell-cell communication and cellular movement genes.** Expression of genes related to cellular movement differentiated IL1RKO from WT and TNFRKO mice at 3 and 5 dpi (Table 3). This included a

TABLE 3. Top 10 IPA canonical pathways that distinguish IL1RKO mice from WT and TNFRKO mice following infection with r1918 influenza virus

| Day | IPA canonical pathway[a] | B-H *P* value[b] |
|---|---|---|
| 1 | Cross talk between DC and NK cells | 1.47E−05 |
| | Hepatic fibrosis/hepatic stellate cell activation | 4.65E−05 |
| | Pancreatic adenocarcinoma signaling | 8.72E−04 |
| | TREM1 signaling | 8.72E−04 |
| | Colorectal cancer metastasis signaling | 9.07E−04 |
| | Atherosclerosis signaling | 3.95E−03 |
| | Glioma signaling | 3.95E−03 |
| | DC maturation | 4.63E−03 |
| | Acute-phase response signaling | 7.39E−03 |
| | DNA methylation and transcriptional repression signaling | 7.73E−03 |
| 3 | Hepatic fibrosis/hepatic stellate cell activation | 7.45E−03 |
| | Nicotinate and nicotinamide metabolism | 1.04E−02 |
| | Tight-junction signaling | 1.76E−02 |
| | Atherosclerosis signaling | 3.09E−02 |
| | Acute-phase response signaling | 3.19E−02 |
| | Polyamine regulation in colon cancer | 4.51E−02 |
| | Colorectal cancer metastasis signaling | 5.34E−02 |
| | Actin cytoskeleton signaling | 5.34E−02 |
| | Aryl hydrocarbon receptor signaling | 5.39E−02 |
| | Pancreatic adenocarcinoma signaling | 5.39E−02 |
| 5 | Hepatic fibrosis/hepatic stellate cell activation | 2.53E−04 |
| | Tight-junction signaling | 4.26E−03 |
| | Actin cytoskeleton signaling | 4.61E−03 |
| | JAK/STAT signaling | 4.71E−03 |
| | ILK signaling | 4.71E−03 |
| | Atherosclerosis signaling | 1.18E−02 |
| | GM-CSF signaling | 1.18E−02 |
| | Integrin signaling | 1.18E−02 |
| | VEGF signaling | 1.18E−02 |
| | AMPK signaling | 1.18E−02 |

[a] Top pathways were determined using IPA of genes that were different by ANOVA using posthoc comparisons to determine pairwise differences in gene expression at each time point. VEGF, vascular endothelial growth factor; GM-CSF, granulocyte-macrophage colony-stimulating factor; AMPK, AMP-activated protein kinase.

[b] A Benjamini-Hochberg (B-H) test correction was applied to significance values for each pathway.

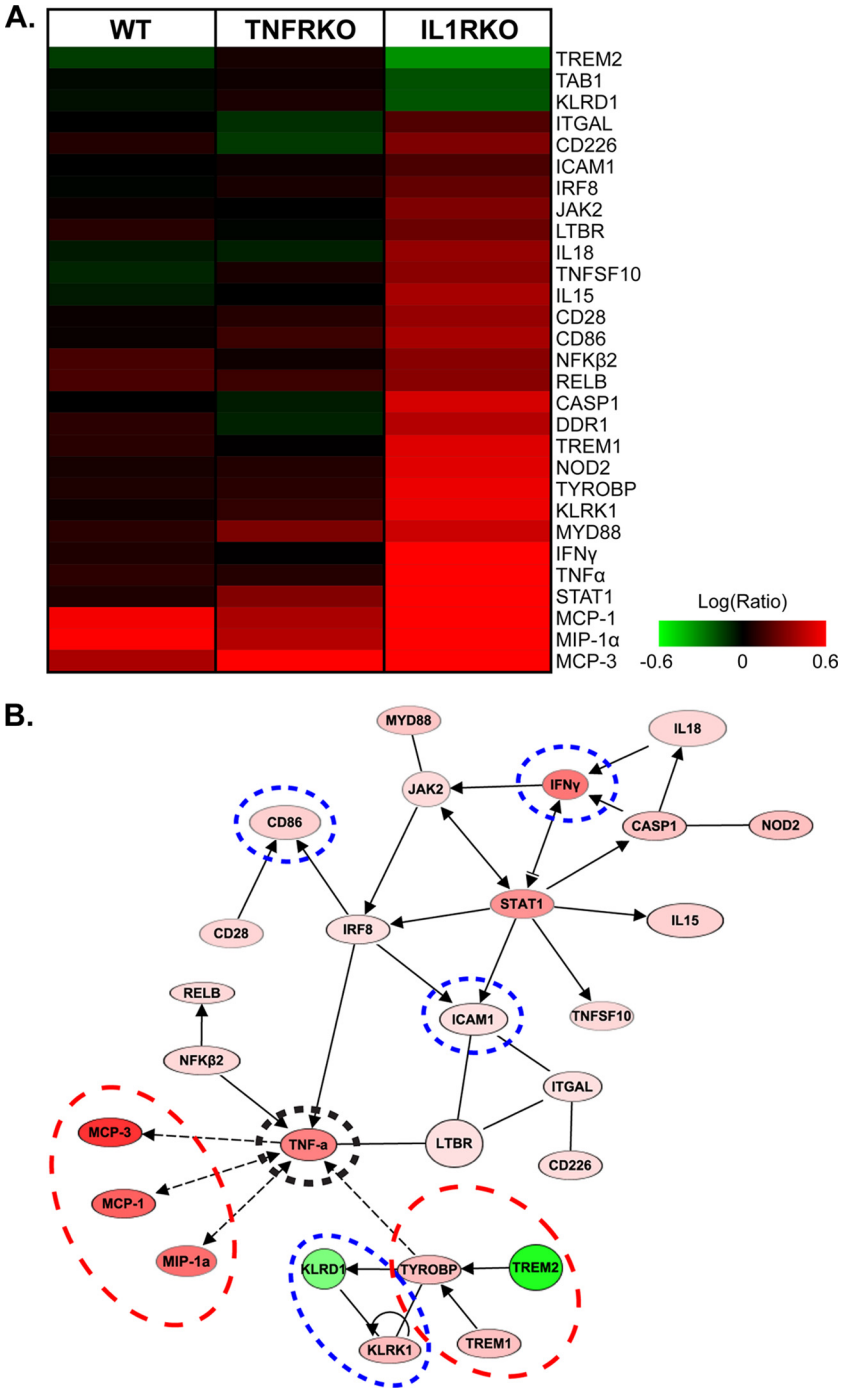


FIG. 6. IL1RKO mice show differential gene expression of TREM signaling-related genes and DC maturation at day 1 postinfection. (A) Expression of genes related to TREM1 and DC signaling was unique in the IL1RKO animals at 1 dpi. Average expression for each group is shown as the log(ratio) of expression relative to a pool of RNA extracted from lungs of mock-infected mice, matched for genetic background to each strain. Red indicates that the gene expression is higher than that in the uninfected reference; green indicates that gene expression is lower than that in the uninfected reference sample. Clustering was performed using a hierarchical unweighted-pair group method using average linkages (UPGMA) with a Euclidean distance similarity measure and average value ordering function. (B) IPA network showing the functional relationships between genes involved in TREM1 signaling, DC maturation, and cross talk between DC and NK cells. Nodes depict genes in the network, and lines represent the relationship between nodes. Solid lines, direct interactions; dashed lines, indirect interactions.

significant number of genes related to tight-junction signaling and actin cytoskeleton signaling at 3 dpi (Fig. 7). In addition to these pathways, there was a significant enrichment of genes related to integrin and integrin-linked kinase (ILK) that distinguished IL1RKO from WT and TNFRKO mice at 5 dpi. Although there were some downregulated genes (CCND1 and DSP) that had the lowest expression in the IL1RKO mice among all strains, in general the expression of the genes related

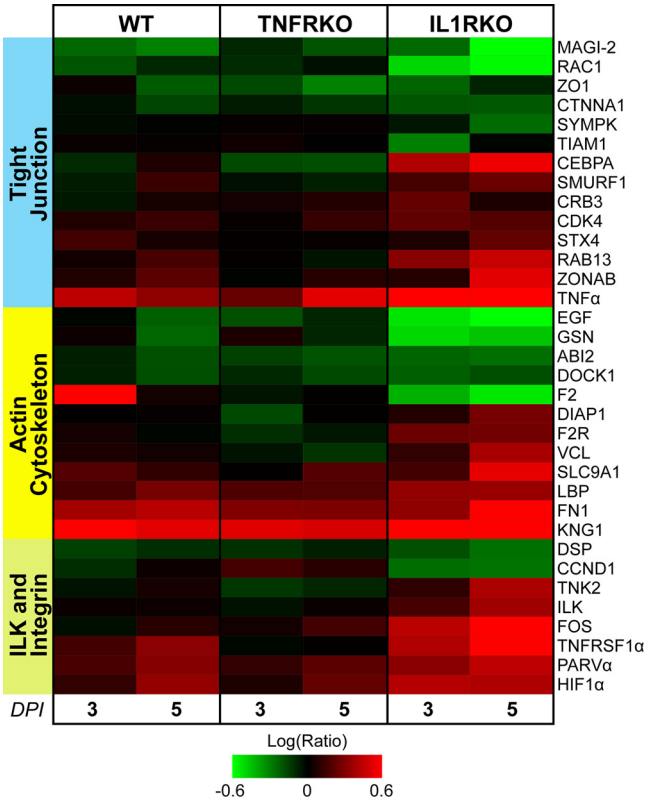


FIG. 7. IL1RKO mice show differential expression of cellular movement genes at 3 and 5 dpi. Transcription of genes related to cellular movement differentiated the IL1RKO mice from WT and TNFRKO mice at 3 and 5 dpi. Two-dimensional clustering of differentially expressed genes within the categories of actin cytoskeleton signaling, tight-junction signaling, and ILK and integrin signaling pathways are represented. Average expression for each group is shown as the log(ratio) of expression relative to a pool of RNA extracted from lungs of mock-infected mice, matched for genetic background to each strain. Red indicates that the gene expression is higher than that in the uninfected reference; green indicates that gene expression is lower than that in the uninfected reference sample. Clustering was performed using a hierarchical unweighted-pair group method using average linkages (UPGMA) with a Euclidean distance similarity measure and average value ordering function.

to both integrin and ILK signaling were upregulated and at 5 dpi had the highest expression in IL1RKO mice.

Highly pathogenic H5N1 avian influenza virus and r1918 pandemic influenza virus infections have a dramatic impact on immune cell infiltration into the mouse lung, causing excessive macrophage and neutrophil infiltration that likely affects immunopathological outcome (24). Our analyses revealed that mice deficient in IL-1R1 signaling show enhanced gene expression changes related to cellular movement and cell-to-cell signaling. These transcriptional events, which influence tight-junction and actin cytoskeleton signaling, precede leukocyte extravasation and infiltration. Integrin and ILK signaling are closely related and play a key role in translating extracellular signals to intracellular changes in signaling and structure. These differences in inflammation and cell-to-cell signaling support our histopathology findings (Fig. 2). The histopathology shows that at day 1 the IL1RKO mice had greater inflammation in the airways, which was accompanied by a higher infiltration of both polymorphonuclear leukocytes (PMN) and histiocytes (HC) than in WT or TNFRKO mice. Interestingly, by day 3 postinfection, the WT mice had more severe inflammation with more PMN and HC than the other two groups. This may suggest that the early increase in infiltration in these mice was a more important determinant of lethality than the later levels of infiltration.

The coordinated expression within these functionally related pathways suggests that a deficiency in IL-1R1 signaling leads to a compensatory increase in proinflammatory signaling at 1 dpi and cell-to-cell communication and movement at 3 and 5 dpi (see Fig. S3 in the supplemental material), which may be due in part to the greater increase in TNF-α gene expression in the IL1RKO mice. In combination with the histopathology data, this may suggest that the combination of early inflammatory response and increased TNF-α-associated signaling contributed to the early mortality in the IL1RKO mice. Overall, we observed that the TNFRKO mice exhibited a decrease in the expression of acute-phase genes and a decrease in the expression of early antiviral genes throughout r1918 virus infection. Combined, these transcriptional data suggest that, despite redundancy in the actions of IL-1 and TNF-α, during r1918 infection these animals show distinct responses that may in part contribute to the accelerated mortality in the IL1RKO mice and delayed mortality in the TNFRKO mice.

## DISCUSSION

Our study is the first to use global gene expression profiling to investigate the differences in the host transcriptional response to r1918 virus infection among WT, IL1RKO, and TNFRKO mouse strains. Despite reported redundancy in the functions of IL-1β and TNF-α, we observed that reducing the signaling capacity of each of these molecules by genetic disruption of their key receptor genes had dramatically different effects on the host response to r1918 virus infection. Further, the present study narrows the hypothesis that a general, augmented proinflammatory cytokine response (cytokine storm) is a critical determinate to the severity of influenza virus infection. That is, the transcriptional data from both the IL1RKO and TNFRKO mice suggest that TNFR signaling is the more critical determinant of the host response to 1918 virus infection.

**Survival, innate immunity, and differential host responses in the TNFRKO and IL1RKO mice.** We observed a trend toward accelerated mortality in the IL1RKO mice and delayed mortality in the TNFRKO mice compared to the WT mice. The increased time to death in the TNFRKO mice may be due to a reduction in morbidity as these mice were able to maintain their body weight longer following infection. In addition, tissue damage in these animals became less severe over time, and TNFRKO mice exhibited the least amount of tissue damage of any strain at 5 dpi. Although tissue damage in the IL1RKO mice also decreased over time, the damage was still greater than in the TNFRKO mice. In contrast, damage to pulmonary tissue increased in WT mice at 3 and 5 dpi. Previous reports of TNFRKO mice infected with an avian-origin influenza H5N1 virus (A/Hong Kong/486/97 or A/Hong Kong/483/97) (30) and IL1RKO mice infected with a mouse-adapted H1N1 virus (A/Puerto Rico/8/34) (27) found that these viruses induced similar

weight loss, lung viral titers, and viral dissemination in WT and knockout mice. Recent studies in macaques (7) and mice (6, 24) have indicated that highly pathogenic avian-origin H5N1 viruses and r1918 incur distinct host responses with regard to the biological pathways differentially regulated during infection, as well as the timing of those responses. Because previous studies of influenza virus infection in TNFRKO and IL1RKO mice did not include global gene expression analysis, further studies are necessary to determine the similarities and differences in transcriptional responses to other highly pathogenic influenza virus strains, including H5N1 viruses.

Using high-throughput technology, we were able to identify alterations in specific biological pathways that were connected with severity of disease. We observed that IL1RKO mice had a similar gross transcriptional response to the virus on each day postinoculation, which was characterized by differential expression of a large number of genes and relatively uniform expression over time. This suggests that IL-1R1 signaling may be necessary for effective modulation of the host transcriptional response to infection.

Our findings also suggest that an increase in gene expression related to interferon signaling during acute infection may be linked to accelerated mortality. Although we observed an upregulation of interferon-related innate signaling following infection with r1918 virus in all three strains of mice, the mice that survived the longest had the lowest overall expression of genes within this network. One of the earliest host responses against influenza virus infection is the activation of innate signaling events that ultimately lead to the induction of interferon and interferon-stimulated genes (reviewed in reference 15). Previously, our group and others have demonstrated that the increased severity of r1918 virus infection in mice was associated with an increased, early interferon transcriptional response (14). These findings suggest that this early response to infection could be useful in the screening to predict the severity of influenza virus infection. A recent study of r1918 virus infection in IFN-α/β-receptor mice found that the absence of functional signaling through these receptors resulted in striking differences in transcriptional profiles and dissemination compared to WT mice infected with r1918 virus (6). Our data suggest that tempering of these antiviral responses by the removal of TNFR signaling may be one factor that contributes to the decrease in pathogenesis of r1918 virus infection in TNFRKO mice.

**Differential regulation of acute phase signaling in KO mice—effect on complement and coagulation pathways.** The acute-phase response to infection results in a wide range of local effects and systemic alterations that are evidenced in changes that are generally proinflammatory, such as the increase in specific cytokine production, and that can be linked to viral clearance, such as increases in complement (reviewed in reference 10). The role of IL-1 and TNF-α in the activation of the acute-phase response is well established. In general, we observed a downregulation of acute-phase signaling in TNFRKO mice compared to the WT and IL1RKO at 1 and 3 dpi, and TNFRKO mice exhibited a delay in the differential expression of genes associated with the complement cascade. In contrast, IL1RKO mice exhibited the highest expression of complement-related genes. Activation of the complement cascade generally acts as a bridge between innate and adaptive immunity, leading to enhanced recruitment and activation of immune cells and formation of the membrane attack complex on infected cells. Our observation that removal of TNFR and IL-1R1 altered expression within the complement pathway is notable because recent studies suggest that activation of antiviral $CD4^+$ and $CD8^+$ T-cell responses, including cytolytic activities, in the lungs of influenza virus-infected mice are associated with complement molecules C3 and C5 (17, 19, 21). Other studies have shown that TNF-α may augment immunopathology in part through a CD8-specific cytotoxic T-lymphocyte (CTL) response at the endothelium of influenza virus-infected tissue (33). We observed that IL1RKO mice exhibited a decrease in the expression of the complement protein C5 gene at 1 dpi compared to WT and TNFRKO mice. These previous findings and our results suggest that further investigation is warranted into the link between influenza virus pathogenesis and activation of the complement cascade.

In addition, we observed that gene expression within the coagulation pathway was significantly lower in TNFRKO mice than in the other mice at 1 and 3 dpi, suggesting a delay or dampening of this response. Studies of H1N1 influenza virus infection in mice have shown that lethal infection coincides with an increase in lung and systemic markers of activated coagulation pathways, suggesting a prothrombic state during infection (16, 28). The reduction in the expression of coagulation-related genes in TNFRKO mice coincided with an increase in survival and a decrease in tissue damage. However, future studies are necessary to determine if these differences in coagulation contribute to the lessened severity of disease in these animals.

Negative acute-phase proteins may play a role in the binding of molecules, such as retinol and cortisol. A decrease in negative acute-phase proteins during infection may create an increase in the bioavailability of such hormones. We observed an increase in the expression of genes coding for negative acute-phase proteins in WT mice. In contrast, we observed that expression of negative acute-phase genes was similar in the IL-1R1 and TNFR mice, whereas the expression was lower than the WT mice. This may suggest that signaling from IL-1 and/or TNF-α is necessary for transcriptional upregulation of these genes. Glucocorticoid steroids, such as cortisol, possess immunomodulatory functions and both regulate and are responsive to proinflammatory cytokines during viral infection (reviewed in references 4 and 29). Based on this reciprocal regulation, these steroids have been investigated as an adjuvant to anti-influenza virus therapies (23). Because the functional repercussions of the decrease in the expression of negative acute-phase genes in this model are unclear, it deserves further study in the future.

**Compensatory and enhanced expression of TNF-α and TREM1 signaling pathways in IL1RKO mice.** Unexpectedly, we observed an increase in TNF-α gene expression in IL1RKO mice, which correlated to increased expression of several downstream pathways and which could explain in part why these mice died sooner than either WT or TNFRKO mice. The increase in TNF-α expression in IL1RKO mice was associated with an increase in inflammatory signaling at 1 dpi and cellular movement pathways at 3 and 5 dpi. The absence of IL-1R1 signaling correlated to the greatest increase in TREM1 signaling and DC maturation and cross talk with NK cells and the

greatest magnitude of gene expression changes in actin cytoskeleton, tight junction, integrin, and ILK signaling at 3 and 5 dpi.

TREM1 is expressed on immune cell populations, including monocytes and neutrophils. Previous reports have shown that TREM1 amplifies inflammation during bacterial (2) and Ebola virus (22) infections in part through the activation of DAP12 signaling pathways and is linked to increased proinflammatory cytokine secretion and survival of neutrophils and monocytes. Our findings related to the TREM1 pathway at 1 dpi are particularly interesting, given the link between this molecule and the host response to other microbial pathogens. The upregulation of genes related to TREM1 signaling in IL1RKO mice may promote a more aggravated inflammatory response earlier during infection, as evidenced by the increased immunopathology of IL1RKO mice at 1 dpi. Although the inflammation in the lung, as evidenced by histopathology, was not the highest in IL1RKO mice at later time points, it is possible that this transcriptional change could impact the level of circulating inflammatory mediators. Alternatively, the increased expression of genes associated with inflammation and antiviral responses in the lungs at 1 dpi in the IL1RKO mice may have triggered an irreversible cascade of events in the lungs that contributed to these mice dying earlier than the other mouse strains.

In conclusion, our results indicate that TNFR signaling increases the severity of 1918 virus infection while IL-1R1 signaling is largely protective. This study presents specific alterations in the host response to infection that may explain in part the differential survival and lung damage observed in our study and in previous studies using these mice (27, 30). In particular, our data suggest that TNF-α signaling may be a key regulator of pathogenesis, as evidenced by both the direct removal of signaling in TNFRKO mice and the compensatory upregulation of transcription of TNF-α in IL1RKO mice. By determining the host signaling pathways connected with pathogenesis, it may be possible to manipulate these pathways for the benefit of vaccine or therapeutic developments. Our findings therefore add to our overall knowledge of influenza virus infection in a way that may ultimately have greater benefit for treatment of the individual and may help us to contain highly pathogenic influenza viruses before their spread reaches pandemic levels.

## ACKNOWLEDGMENTS

This study was funded in part by Public Health Service grant P01AI058113 from the National Institute of Allergy and Infectious Diseases.

The findings and conclusions in this report are those of the authors and do not necessarily represent the views of the Centers for Disease Control and Prevention.

## REFERENCES

1. **Beigel, J. H., J. Farrar, A. M. Han, F. G. Hayden, R. Hyer, M. D. de Jong, S. Lochindarat, T. K. Nguyen, T. H. Nguyen, T. H. Tran, A. Nicoll, S. Touch, and K. Y. Yuen.** 2005. Avian influenza A (H5N1) infection in humans. N. Engl. J. Med. **353:**1374–1385.
2. **Bouchon, A., F. Facchetti, M. A. Weigand, and M. Colonna.** 2001. TREM-1 amplifies inflammation and is a crucial mediator of septic shock. Nature **410:**1103–1107.
3. **Brazma, A., P. Hingamp, J. Quackenbush, G. Sherlock, P. Spellman, C. Stoeckert, J. Aach, W. Ansorge, C. A. Ball, H. C. Causton, T. Gaasterland, P. Glenisson, F. C. Holstege, I. F. Kim, V. Markowitz, J. C. Matese, H. Parkinson, A. Robinson, U. Sarkans, S. Schulze-Kremer, J. Stewart, R. Taylor, J. Vilo, and M. Vingron.** 2001. Minimum information about a microarray experiment (MIAME)—toward standards for microarray data. Nat. Genet. **29:**365–371.
4. **Carter, M. J.** 2007. A rationale for using steroids in the treatment of severe cases of H5N1 avian influenza. J. Med. Microbiol. **56:**875–883.
5. **Chomczynski, P., and N. Sacchi.** 1987. Single-step method of RNA isolation by acid guanidinium thiocyanate-phenol-chloroform extraction. Anal. Biochem. **162:**156–159.
6. **Cilloniz, C., M. J. Pantin-Jackwood, C. Ni, A. G. Goodman, X. Peng, S. C. Proll, V. C. Carter, E. R. Rosenzweig, K. J. Szretter, J. M. Katz, M. J. Korth, D. E. Swayne, T. M. Tumpey, and M. G. Katze.** 2010. Lethal dissemination of H5N1 influenza virus is associated with dysregulation of inflammation and lipoxin signaling in a mouse model of infection. J. Virol. **84:**7613–7624.
7. **Cilloniz, C., K. Shinya, X. Peng, M. J. Korth, S. C. Proll, L. D. Aicher, V. S. Carter, J. H. Chang, D. Kobasa, F. Feldmann, J. E. Strong, H. Feldmann, Y. Kawaoka, and M. G. Katze.** 2009. Lethal influenza virus infection in macaques is associated with early dysregulation of inflammatory related genes. PLoS Pathog. **5:**e1000604.
8. **de Jong, M. D., C. P. Simmons, T. T. Thanh, V. M. Hien, G. J. Smith, T. N. Chau, D. M. Hoang, N. V. Chau, T. H. Khanh, V. C. Dong, P. T. Qui, B. V. Cam, Q. Ha do, Y. Guan, J. S. Peiris, N. T. Chinh, T. T. Hien, and J. Farrar.** 2006. Fatal outcome of human influenza A (H5N1) is associated with high viral load and hypercytokinemia. Nat. Med. **12:**1203–1207.
9. **Dinarello, C. A.** 2009. Immunological and inflammatory functions of the interleukin-1 family. Annu. Rev. Immunol. **27:**519–550.
10. **Gabay, C., and I. Kushner.** 1999. Acute-phase proteins and other systemic responses to inflammation. N. Engl. J. Med. **340:**448–454.
11. **Ginsburg, G. S., J. Ozer, and S. K. Karathanasis.** 1995. Intestinal apolipoprotein AI gene transcription is regulated by multiple distinct DNA elements and is synergistically activated by the orphan nuclear receptor, hepatocyte nuclear factor 4. J. Clin. Invest. **96:**528–538.
12. **Herbein, G., and W. A. O'Brien.** 2000. Tumor necrosis factor (TNF)-alpha and TNF receptors in viral pathogenesis. Proc. Soc. Exp. Biol. Med. **223:** 241–257.
13. **Johnson, N. P., and J. Mueller.** 2002. Updating the accounts: global mortality of the 1918–1920 "Spanish" influenza pandemic. Bull. Hist Med. **76:** 105–115.
14. **Kash, J. C., T. M. Tumpey, S. C. Proll, V. Carter, O. Perwitasari, M. J. Thomas, C. F. Basler, P. Palese, J. K. Taubenberger, A. Garcia-Sastre, D. E. Swayne, and M. G. Katze.** 2006. Genomic analysis of increased host immune and cell death responses induced by 1918 influenza virus. Nature **443:**578–581.
15. **Katze, M. G., J. L. Fornek, R. E. Palermo, K. A. Walters, and M. J. Korth.** 2008. Innate immune modulation by RNA viruses: emerging insights from functional genomics. Nat. Rev. Immunol. **8:**644–654.
16. **Keller, T. T., K. F. van der Sluijs, M. D. de Kruif, V. E. Gerdes, J. C. Meijers, S. Florquin, T. van der Poll, E. C. van Gorp, D. P. Brandjes, H. R. Buller, and M. Levi.** 2006. Effects on coagulation and fibrinolysis induced by influenza in mice with a reduced capacity to generate activated protein C and a deficiency in plasminogen activator inhibitor type 1. Circ. Res. **99:**1261–1269.
17. **Kim, A. H., I. D. Dimitriou, M. C. Holland, D. Mastellos, Y. M. Mueller, J. D. Altman, J. D. Lambris, and P. D. Katsikis.** 2004. Complement C5a receptor is essential for the optimal generation of antiviral $CD8^+$ T cell responses. J. Immunol. **173:**2524–2529.
18. **Kobasa, D., S. M. Jones, K. Shinya, J. C. Kash, J. Copps, H. Ebihara, Y. Hatta, J. H. Kim, P. Halfmann, M. Hatta, F. Feldmann, J. B. Alimonti, L. Fernando, Y. Li, M. G. Katze, H. Feldmann, and Y. Kawaoka.** 2007. Aberrant innate immune response in lethal infection of macaques with the 1918 influenza virus. Nature **445:**319–323.
19. **Kopf, M., B. Abel, A. Gallimore, M. Carroll, and M. F. Bachmann.** 2002. Complement component C3 promotes T-cell priming and lung migration to control acute influenza virus infection. Nat. Med. **8:**373–378.
20. **Labow, M., D. Shuster, M. Zetterstrom, P. Nunes, R. Terry, E. B. Cullinan, T. Bartfai, C. Solorzano, L. L. Moldawer, R. Chizzonite, and K. W. McIntyre.** 1997. Absence of IL-1 signaling and reduced inflammatory response in IL-1 type I receptor-deficient mice. J. Immunol. **159:**2452–2461.
21. **Longhi, M. P., A. Williams, M. Wise, B. P. Morgan, and A. Gallimore.** 2007. CD59a deficiency exacerbates influenza-induced lung inflammation through complement-dependent and -independent mechanisms. Eur. J. Immunol. **37:**1266–1274.
22. **Mohamadzadeh, M., S. S. Coberley, G. G. Olinger, W. V. Kalina, G. Ruthel, C. L. Fuller, D. L. Swenson, W. D. Pratt, D. B. Kuhns, and A. L. Schmaljohn.** 2006. Activation of triggering receptor expressed on myeloid cells-1 on human neutrophils by Marburg and Ebola viruses. J. Virol. **80:**7235–7244.
23. **Ottolini, M., J. Blanco, D. Porter, L. Peterson, S. Curtis, and G. Prince.** 2003. Combination anti-inflammatory and antiviral therapy of influenza in a cotton rat model. Pediatr. Pulmonol. **36:**290–294.
24. **Perrone, L. A., J. K. Plowden, A. Garcia-Sastre, J. M. Katz, and T. M. Tumpey.** 2008. H5N1 and 1918 pandemic influenza virus infection results in early and excessive infiltration of macrophages and neutrophils in the lungs of mice. PLoS Pathog. **4:**e1000115.
25. **Peschon, J. J., D. S. Torrance, K. L. Stocking, M. B. Glaccum, C. Otten, C. R. Willis, K. Charrier, P. J. Morrissey, C. B. Ware, and K. M. Mohler.** 1998.

TNF receptor-deficient mice reveal divergent roles for p55 and p75 in several models of inflammation. J. Immunol. **160:**943–952.
26. **Sabbah, A., T. H. Chang, R. Harnack, V. Frohlich, K. Tominaga, P. H. Dube, Y. Xiang, and S. Bose.** 2009. Activation of innate immune antiviral response by NOD2. Nat. Immunol. **10:**1073–1080.
27. **Schmitz, N., M. Kurrer, M. F. Bachmann, and M. Kopf.** 2005. Interleukin-1 is responsible for acute lung immunopathology but increases survival of respiratory influenza virus infection. J. Virol. **79:**6441–6448.
28. **Schouten, M., K. F. van der Sluijs, B. Gerlitz, B. W. Grinnell, J. J. Roelofs, M. M. Levi, C. van 't Veer, and T. V. Poll.** 2010. Activated protein C ameliorates coagulopathy but does not influence outcome in lethal H1N1 influenza: a controlled laboratory study. Crit. Care **14:**R65.
29. **Silverman, M. N., B. D. Pearce, C. A. Biron, and A. H. Miller.** 2005. Immune modulation of the hypothalamic-pituitary-adrenal (HPA) axis during viral infection. Viral Immunol. **18:**41–78.
30. **Szretter, K. J., S. Gangappa, X. Lu, C. Smith, W. J. Shieh, S. R. Zaki, S. Sambhara, T. M. Tumpey, and J. M. Katz.** 2007. Role of host cytokine responses in the pathogenesis of avian H5N1 influenza viruses in mice. J. Virol. **81:**2736–2744.
31. **Tumpey, T. M., C. F. Basler, P. V. Aguilar, H. Zeng, A. Solorzano, D. E. Swayne, N. J. Cox, J. M. Katz, J. K. Taubenberger, P. Palese, and A. Garcia-Sastre.** 2005. Characterization of the reconstructed 1918 Spanish influenza pandemic virus. Science **310:**77–80.
32. **Turnbull, I. R., S. Gilfillan, M. Cella, T. Aoshi, M. Miller, L. Piccio, M. Hernandez, and M. Colonna.** 2006. Cutting edge: TREM-2 attenuates macrophage activation. J. Immunol. **177:**3520–3524.
33. **Xu, L., H. Yoon, M. Q. Zhao, J. Liu, C. V. Ramana, and R. I. Enelow.** 2004. Cutting edge: pulmonary immunopathology mediated by antigen-specific expression of TNF-alpha by antiviral $CD8^+$ T cells. J. Immunol. **173:**721–725.